

Original Research Article

Structural, electrical and magnetic study of $\text{BiNi}_x\text{Fe}_{1-x}\text{O}_3$ ($x=0-1$) spin-coated ferrite films

ABSTRACT

Aims: To fabricate $\text{BiNi}_x\text{Fe}_{1-x}\text{O}_3$ ($x=0-1$) ferrite films on a Si substrate with a thin Pt buffer using the spin coating method.

Study design: The focus of the study was two-fold: to examine the properties of the $\text{BiNi}_x\text{Fe}_{1-x}\text{O}_3$ ($x=0-1$) family of materials and to determine whether Pt is a suitable element for preventing diffusion between the film and the substrate.

Place and Duration of Study: Dept. of Physics and Dept. of Electrical & Computer Engineering, Aristotle University of Thessaloniki and Dept. of Materials Science and Engineering, University of Ioannina, between November 2019 and November 2021.

Methodology: The films were manufactured with the spin-coating method, and characterization was performed with various methods, including XRD, SEM/EDAX and VSM measurements

Results: Pt can prevent diffusion effects. The target material was not formed, probably due to the low annealing temperature. No magnetoelectric properties were detected.

Conclusion: The spin-coating method is not recommended for the fabrication of these materials.

Keywords: spin coating, magnetic measurements, magnetoelectric properties

1. INTRODUCTION

Magnetoelectric (ME) materials have attracted a lot of attention lately, mainly because their intrinsic properties enable the control of the magnetic state through the application of an electric signal, and vice versa. The realization of this effect would lead to a slew of applications, such as fast magnetoelectric RAM, highly sensitive magnetic sensors in the pTesla range, spin-valves and more [1-3].

Research interest has mainly focused on the BiFeO_3 perovskite (BFO), since it is one of the few materials that exhibits both ferroelectricity and magnetic ordering in room temperature [4-6]. Also, there have been attempts to study the effect of various substituting elements, such as Co, Cr, Mn, Cu for Fe and La for Bi [7-12], in the microstructure and intrinsic properties of the material with varying results. However, these attempts focus on small percentages of substitutions.

Attempts to enhance the magnetoelectric properties of BFO through epitaxial strain have succeeded, producing thin films with excellent properties, however these films demand the use of intermediate layers of oxides such as SrRuO_3 , SrTiO_3 και LaAlO_3 , thus increasing significantly the production costs [13-16]. On the other hand, growth of BFO films directly on a Si substrate produces films with poor magnetoelectric properties. Also, it appears that there is significant diffusion between film and substrate [17].

In this work, we attempted the synthesis of $\text{BiNi}_x\text{Fe}_{1-x}\text{O}_3$ ($x=0-1$) (BNFO) thin films on a Si substrate using the spin-coating method and the study of the structural, magnetic and electrical properties of the entire family with various experimental methods. Also, we examine the use of a Pt buffer layer between film and Si as a method of eliminating diffusion problems.

2. MATERIAL AND METHODS / EXPERIMENTAL DETAILS / METHODOLOGY

2.1 Chemical preparation and annealing procedure

The BNFO films were manufactured using the spin-coating method, which is a well-known and practiced method for depositing ceramic materials on substrates [18]. The sol-gel method [19] was used to create the necessary precursor materials, as described in detail below.

An aqueous solution of appropriate quantities of $\text{Bi}(\text{NO}_3)_3 \cdot 5\text{H}_2\text{O}$, $\text{Fe}(\text{NO}_3)_3 \cdot 9\text{H}_2\text{O}$ and $\text{Ni}(\text{NO}_3)_2 \cdot 6\text{H}_2\text{O}$ was mixed in a magnetic stirrer. After the solution was stirred and heated at 80°C , citric acid was added and the mixture was heated at 85°C . Then, ethylene glycol was added. The pH of the mixture was monitored so as not to fall below 10. The mixture was stirred at 85°C until the water evaporated and a gel was formed.

Consequently, the gel was applied on Si wafers capped with a thin (100nm) Pt layer. The purpose of the Pt layer was two-fold: to prevent the diffusion of the BNFO into the substrate, and to provide a base crystal structure for the growth of the films because of the similar cell dimensions of Pt and BFO. The gel was rotated at 4000-5000rpm for 60 sec and dried at 170°C for 10mins, in order to dispose of the excess ethylene glycol. Once the gel was dried sufficiently, the films were annealed in air at 600°C for 4h in order to form the main phase. No attempts were made in higher annealing temperatures, because of the tendency of Pt to form Pt-Si compounds. The entire process is shown in Fig. 1.

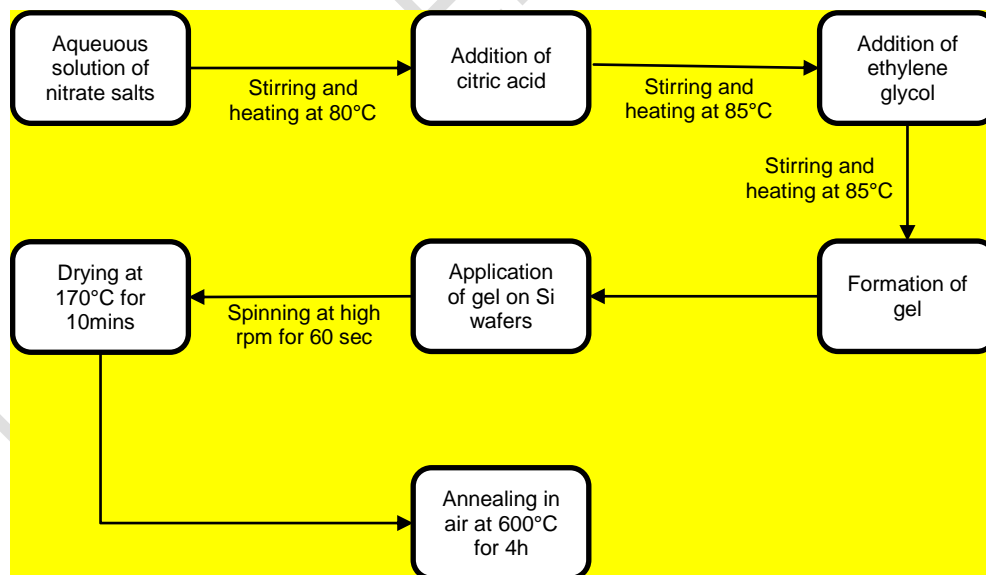


Fig. 1. Chemical preparation and annealing procedure

2.2 Experimental setup

The atomic composition of the calcined powders was evaluated by means of a JEOL JSM5900A scanning electron microscope, equipped with an INCA x-sight detector (Oxford

Instruments) for energy dispersive X-ray microanalysis. X-ray patterns were obtained by a powder diffractometer (Seifert XRD-3003TT) using CuK_α radiation and were identified according to the relevant JCPDS-ICDD Powder Diffraction Files. The magnetic characterization up to 1.2T was performed with a Vibrating Sample Magnetometer (P.A.R. 155) at room temperature. The electric characterization up to 9V/m was performed with an RT66B Ferroelectric Tester at room temperature.

3. RESULTS AND DISCUSSION

3.1 Structural properties

SEM/EDXS characterization showed that all the samples display the nominal composition with a margin of error <1.5%, as shown on table 1. Fig. 2 shows typical SEM images captured for various compositions.

Table 1. Nominal and measured compositions of materials used

| Ni content | Bi | | Ni | | Fe | |
|------------|---------|----------|---------|----------|---------|----------|
| | Nominal | Measured | Nominal | Measured | Nominal | Measured |
| 0.1 | 50% | 48,27% | 5% | 5,38% | 45% | 48,35% |
| 0.2 | 50% | 48,78% | 10% | 10,44% | 40% | 40,78% |
| 0.3 | 50% | 47,89% | 15% | 15,23% | 35% | 36,88% |
| 0.4 | 50% | 49,36% | 20% | 20,16% | 30% | 30,48% |
| 0.5 | 50% | 48,54% | 25% | 25,26% | 25% | 26,33% |
| 0.6 | 50% | 49,78% | 30% | 30,33% | 20% | 19,89% |
| 0.7 | 50% | 49,14% | 35% | 35,60% | 15% | 15,26% |
| 0.8 | 50% | 48,82% | 40% | 41,24% | 10% | 9,94% |
| 0.9 | 50% | 49,42% | 45% | 45,92% | 5% | 4,66% |
| 1 | 50% | 49,94% | 50% | 50,06% | - | - |

There appears to be a slight underrepresentation of Bi in the films, which can be attributed to the drying and spin-coating processes.

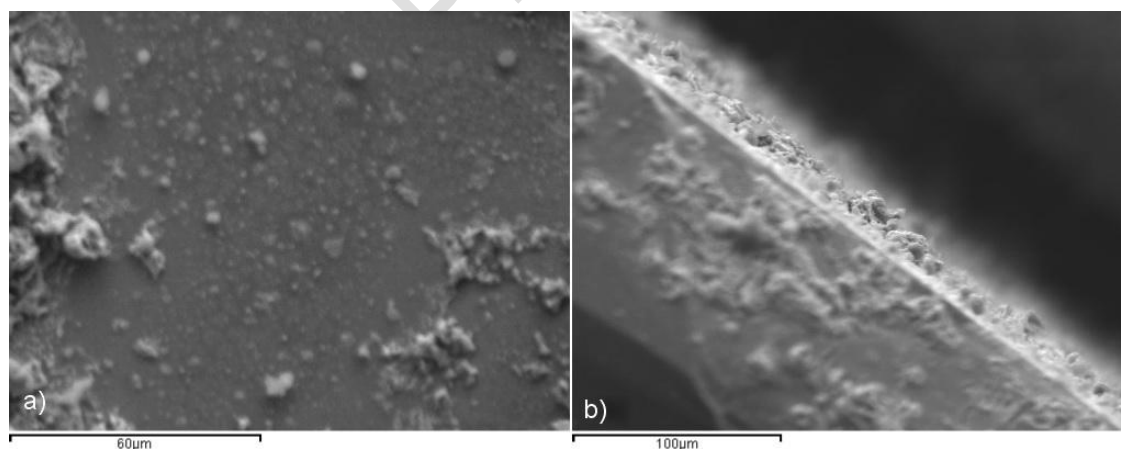


Fig. 2. SEM images of spin-coated BNFO films: a) Surface, b) side of film

From the side images captured, the films' thickness was evaluated between 1-2 μm , which is consistent with the deposition method. Attempts to produce thinner films were not successful: the films were not uniformly deposited and presented with significant cracks and/or empty substrate areas. Also, from the images taken no diffusion appears between the film and the substrate.

In figure 3, the recorded XRD spectra for each composition is presented in ascending order. Pt and Si peaks are indexed accordingly.

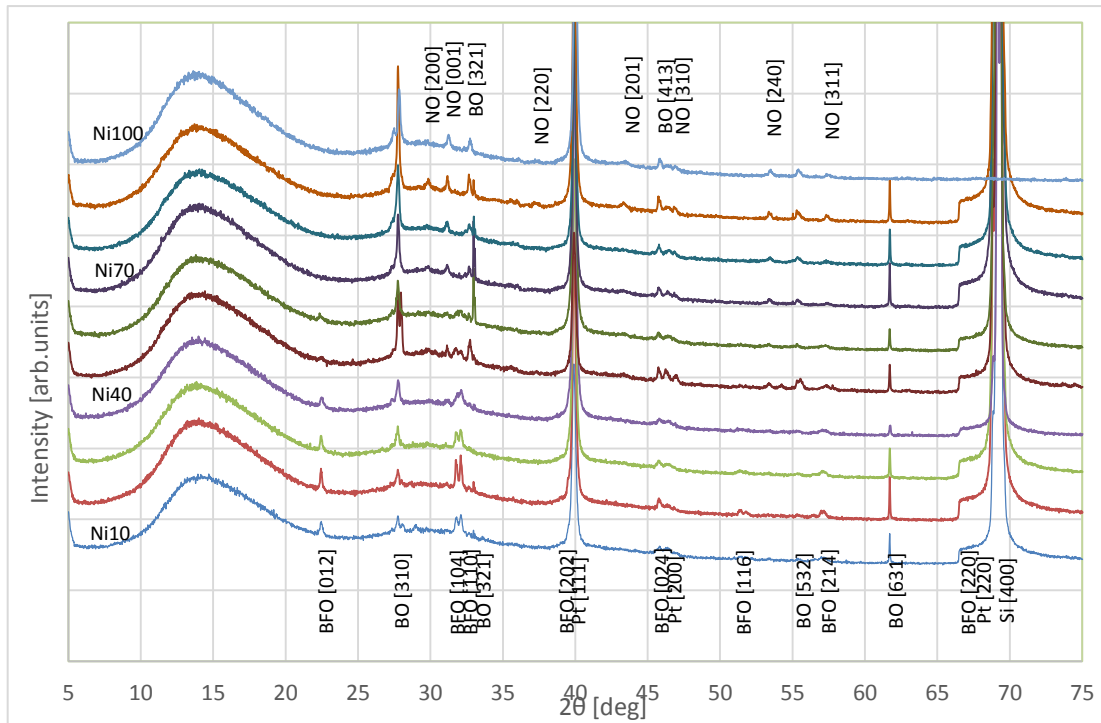


Fig. 3. XRD patterns of BNFO films with different compositions

At low Ni concentration, the material consists of a mix of bismuth ferrite (BFO) and γ - Bi_2O_3 (bismuth oxide, BO). BFO peaks match the rhombohedrally distorted perovskite phase reported by Moreau et al. [20] while BO peaks match the structure reported by Radaev et al. [21], but Rietveld analysis indicates that the cell dimensions are slightly reduced compared to the report. This can be explained by the replacement of a small percentage of Bi by Ni. Cell dimensions increase with increasing Ni content: for 10% Ni, $a=0.10187(4)\text{nm}$ and for 90% Ni, $a=0.10231(3)\text{nm}$. This increase indicates that Ni stops replacing Bi in bismuth oxide, and instead forms another compound, as shown by the appearance of new peaks in Ni concentrations of 50% and above. These peaks are noted as NO (nickel oxide) and match with the Ni_3O_4 orthorhombic structure (Cmmm, $a=0.5984\text{nm}$, $b=0.8263\text{nm}$, $c=0.2879\text{nm}$, $\alpha=\beta=\gamma=90^\circ$). BFO peaks also decrease in intensity and disappear entirely at 60% Ni. At 100% Ni, the film consists entirely of Ni_3O_4 and γ - Bi_2O_3 .

The results indicate that a pure BNFO phase was not formed, which can be attributed to the low annealing temperature. Although there are very few publications concerning partial substitution of Fe by Ni, Ishiwata et al. [22] reported that pure BiNiO_3 was formed under pressure and at much higher temperatures. A future point of research interest would be the use of Si wafers with a SiO_2 oxide layer, thus preventing the formation of PtSi compounds and enabling annealing at higher temperatures.

3.2 Major polarization loops

Major polarization loops were recorded at a maximum electric field of 9V/m at non-magnetized samples. Then, the samples were placed in a DC magnetic field of 1T for several

minutes, and the polarization loops were recorded again. The results of these measurements are shown on Fig.4.

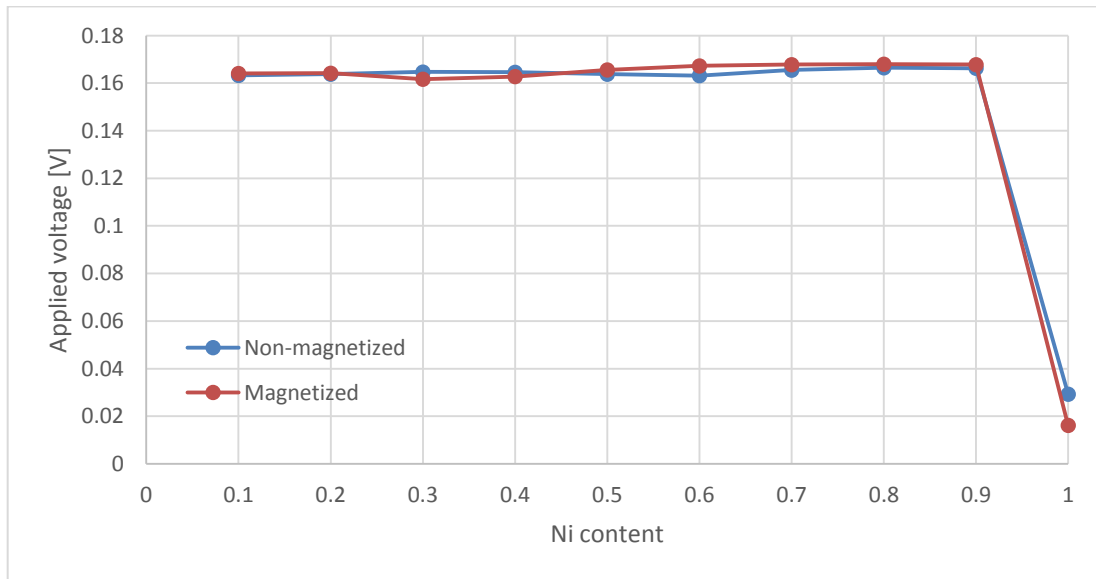


Fig. 4. Applied reversal voltage vs. Ni concentration

The data show that there is no apparent change in the films' electric behavior with increasing Ni content up to 90%. This behavior indicates that ferroelectricity can be attributed to the presence of variable valence Fe ions (Fe^{+2} - Fe^{+3}) in BFO. At 100% Ni, the coercivity practically disappears. Also, the presence of the intrinsic magnetic field has no effect on the electric coercive field.

3.3 Major magnetization loops

Major magnetization loops were recorded at a maximum of 1.2T. In figure 5, the magnetic coercive field for each composition is presented.

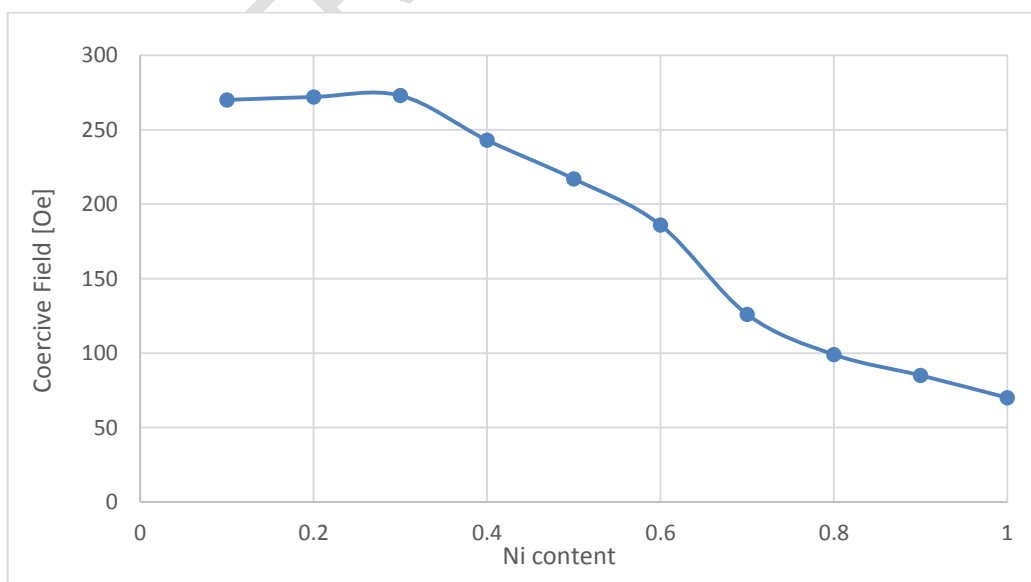


Fig. 5. Coercive magnetic field vs. Ni concentration

The magnetic coercive field is almost constant up to 30% Ni, and then decreases steadily, which corroborates the findings of the structural analysis. To elaborate, the initial coercivity can be attributed to the presence of BFO.

BFO is naturally antiferromagnetic, but mechanical defects and small amounts of impurities in the structure can lead to the appearance of macroscopic ferrimagnetism either through misalignment of Fe spins or through superexchange phenomena between $\text{Fe}^{+2}\text{-O-Fe}^{+3}$ ions [6,7]. With increasing Ni content, BFO begins disappearing, which accounts for the constant decrease in coercivity. At 100% Ni, the coercivity can be attributed to the small percentage of Ni in Bi_2O_3 , which will produce a small magnetic moment in the compound.

4. CONCLUSION

While Pt has proven to be useful in inhibiting diffusion phenomena between Si and BFO, the annealing procedure followed in this study was not successful in producing a distinct $\text{BiNi}_x\text{Fe}_{1-x}\text{O}_3$ phase with distinctive characteristics. The temperature constraints posed by the presence of Pt proved to be incompatible with the spin-coating method, and the final result was that films were composed by different Ni and Bi oxides. However, it is possible that the use of a Si wafer with an oxide layer will produce better results.

ACKNOWLEDGEMENTS

This research is co-financed by Greece and the European Union (European Social Fund-ESF) through the Operational Programme «Human Resources Development, Education and Lifelong Learning» in the context of the project “Reinforcement of Postdoctoral Researchers - 2nd Cycle” (MIS-5033021), implemented by the State Scholarships Foundation (IKY).



REFERENCES

1. Fiebig M. Revival of the magnetoelectric effect, J. of Phys. D: Appl. Phys. 2005;38:R123. <https://doi.org/10.1088/0022-3727/38/8/R01>
2. Gajek M, Bibes M, Fusil S et al. Tunnel junctions with multiferroic barriers, Nature Mat. 2007;6:296. <https://doi.org/10.1038/nmat1860>
3. Ramesh R, Spaldin NA. Multiferroics: progress and prospects in thin films, Nature Mat. 2007;6:21. <https://doi.org/10.1038/nmat1805>
4. Fischer P, Polomska M, Sosnowska I, Szymanski M. Temperature dependence of the crystal and magnetic structures of BiFeO_3 , J. of Phys. C 1980;13:1931. <https://doi.org/10.1088/0022-3719/13/10/012>
5. Michel C, Moreau JM, Achenbechi GD, Gerson R, James WJ. The atomic structure of BiFeO_3 , Sol. St. Comm. 1969;7:701. [https://doi.org/10.1016/0038-1098\(69\)90597-3](https://doi.org/10.1016/0038-1098(69)90597-3)

6. Catalan G, Scott JF. Physics and Applications of Bismuth Ferrite, *Adv. Mater.* 2009;21:2463. <https://doi.org/10.1002/adma.200802849>
7. Kanjariya PV, Bhalodia JA. Correlation of sintering temperature with structural and multiferroic properties of un-doped and cobalt doped bismuth ferrite, *Cer. Int.* 2018;44:14563. <https://doi.org/10.1016/j.ceramint.2018.05.077>
8. Allibe J et al. Coengineering of ferroelectric and exchange bias properties in BiFeO₃ based heterostructures, *Appl. Phys. Lett.* 2009;95:182503. <https://doi.org/10.1063/1.3247893>
9. Guo B et al. Cr doping-induced structural phase transition, optical tuning and magnetic enhancement in BiFeO₃ thin films, *Mater. Lett.* 2017;186:198. <https://doi.org/10.1016/j.matlet.2016.09.094>
10. Hojo H, Onuma K, Ikuhara Y, Azuma M. Structural evolution and enhanced piezoresponse in cobalt-substituted BiFeO₃ thin films, *Appl. Phys. Expr.* 2014;7:091501. <https://doi.org/10.7567/APEX.7.091501>
11. Jampreecha T et al. Studies on structural characterization and electrical properties of Cu-doped BiFeO₃ thin films, *J. Phys.: Conf. Ser.* 2018;1144:012155. <https://doi.org/10.1088/1742-6596/1144/1/012155>
12. Lee YH, Wu JM, Lai CH. Influence of La doping in multiferroic properties of BiFeO₃ thin films, *Appl. Phys. Lett.* 2006;88:042903. <https://doi.org/10.1063/1.2167793>
13. Das RR, Kim DM, Baik SH, Eom CB. Synthesis and ferroelectric properties of epitaxial BiFeO₃ thin films grown by sputtering, *Appl. Phys. Lett.* 2006;88:242904. <https://doi.org/10.1063/1.2213347>
14. Béa H, Gajek M, Bibes M, Barthélémy A. Spintronics with multiferroics, *J. Phys.: Condens. Matter* 2008;20:434221. <https://doi.org/10.1088/0953-8984/20/43/434221>
15. Nakamura Y et al. Enhanced piezoelectric constant of (1-x)BiFeO₃-xBiCoO₃ thin films grown on LaAlO₃ substrate, *Jap. J. of Appl. Phys.* 2011;50:031505. <https://doi.org/10.1143/JJAP.50.031505>
16. Wu J, Xiao D, Zhu J. Effect of La and Co-doping on microstructure and electrical properties of BiFeO₃ thin films, *Chin. Sci. Bull.* 2014;59:5205–5211. <https://doi.org/10.1007/s11434-014-0638-2>
17. Simões AZ et al. Effect of annealing atmosphere on phase formation and electrical characteristics of bismuth ferrite thin films, *Mater. Res. Bull.* 2009;44:1747. <http://dx.doi.org/10.1016/j.materresbull.2009.03.011>
18. Scriven LE, Physics and applications of dip coating and spin coating, *MRS Online Proc. Lib.* 1988;121:717–729. <https://doi.org/10.1557/PROC-121-717>
19. Hench LL, West JK, The sol-gel process, *Chem. Rev.* 90;1990:33–72. <https://doi.org/10.1021/cr00099a003>
20. Moreau J, Michel C, Gerson R, James W. Ferroelectric BiFeO₃ X-Ray and neutron diffraction study, *J. of Phys. Chem. Sol.* 1971;32:1315-1320. [https://doi.org/10.1016/S0022-3697\(71\)80189-0](https://doi.org/10.1016/S0022-3697(71)80189-0)

21. Radaev SF, Simonov VI, Kargin YF. Structural features of γ -phase Bi_2O_3 and its place in the sillenite family, Acta Cryst. 1992;B48:604-609.
<https://doi.org/10.1107/S0108768192003847>

22. Ishiwata S et al. High pressure synthesis, crystal structure and physical properties of a new Ni(II) perovskite BiNiO_3 , J. Mater. Chem. 2002;12:3733–3737.
<https://doi.org/10.1039/B206022A>

UNDER PEER REVIEW